NEAR-FIELD SOUND PROPAGATION BASED ON A CIRCULAR AND LINEAR ARRAY COMBINATION

Takuma Okamoto

National Institute of Information and Communications Technology
3-5, Hikaridai, Seika-cho, Soraku-gun, Kyoto, 619-0289, Japan
okamoto@nict.go.jp

ABSTRACT

This paper proposes a new method for realizing 3D near-field sound propagation. Its main concept is that the sound pressure radiated from a circular sound source outside the circle is completely canceled out using another linear sound source. The appropriate driving functions and the reproduced sound pressures of both sound sources are analytically derived based on the two-dimensional spatial Fourier transform. The radiation property reproduced by a circular source outside the circle is different from that inside the circle. As a result, three-dimensional near-field sound propagation can be realized within the radius of a circular source because the total radiated sound pressure outside the circle can only be completely canceled out. Compared with previous methods, the propagation distance can be controlled by changing the circle's radius. The results of computer simulations suggest that the proposed method can realize effective three-dimensional near-field sound propagation.

Index Terms— Near-field sound propagation, circular loudspeaker array, linear loudspeaker array, spatial Fourier transform, helical wave spectrum

1. INTRODUCTION

Personalizing a listening area is one important and attractive acoustic communication technique. By the superposition of various localized listening areas, multiple listening zones can also be realized [1,2]. These techniques are useful not only for personal sound systems [2–6] but also for multilingual guide services and other virtual reality applications.

There are two active control approaches of a sound field for personalizing a listening area. A number of methods have been proposed that control both the acoustic contrast or the energy between two spaces [1,2,4–10] and reproduce multiple sound fields [11–16] using multiple loudspeakers. In these approaches, the control areas are typically set away from the loudspeakers. In another approach [17–20], a localized sound area is generated near the loudspeakers so that the reproduced sound is only propagated near them, and the sound energy is quite low apart from the loudspeakers. In this paper, the latter approach is called near-field sound propagation.

Some methods of near-field sound propagation have been proposed [17–20]. One is based on evanescent wave [21] reproduction using linear or circular arrays of loudspeakers [17, 18]. In this method, however, the attenuation property of the radiated sound cannot be controlled because the propagation property of the evanescent wave is dependent on the wave length [21]. Another method [19, 20], which uses double circular arrays, is based on least squares approaches [2, 4–7, 9, 11–14]. However, such methods are quite unstable because the acoustic inverse problem is very ill-conditioned [21] and only consider two-dimensional reproduction.

To solve these problems, this paper proposes a new approach for achieving three-dimensional near-field sound propagation. The primary concept of the proposed method is that the sound pressure radiated from a circular sound source outside the circle is completely canceled out using another linear sound source. To realize this situation, an adequate arrangement of both circular and linear sound sources are firstly proposed. Then the appropriate driving functions of the sound sources and the three-dimensional reproduced sound pressures are analytically derived from the analytical approaches of the sound field reproduction based on the two-dimensional spatial Fourier transform [21, 22] and the spectral division method (SDM) [23]. The key point is that the radiation property reproduced by a circular source outside the circle is different from that inside the circle, and the total radiated sound pressure outside the circle can only be perfectly canceled out.

Compared with previous methods [17–20], the propagation distance can be controlled by changing the radius of a circular source, and the driving functions of both the circular and linear sources are based on analytical solutions instead of the least squares approach.

This study was partly supported by JSPS KAKENHI Grant Number 25871208.

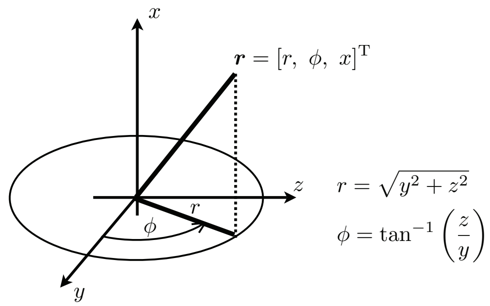

Fig. 1. Definition of cylindrical coordinates $[r,\ \phi,\ x]^{\mathrm{T}}$ relative to Cartesian coordinates $[x,\ y,\ z]^{\mathrm{T}}$.

2. SOUND FIELD REPRODUCED BY CONTINUOUS CYLINDRICAL SECONDARY SOURCE

For describing three-dimensional sound propagation by a continuous circular sound source in the next section, the reproduced sound field by a continuous cylindrical secondary source is briefly introduced.

Cylindrical coordinates $[r,\ \phi,\ x]^{\mathrm{T}}$ relative to Cartesian coordinates $[x,\ y,\ z]^{\mathrm{T}}$ are defined in Fig. 1. Sound pressure $P(\boldsymbol{r},\omega)$ synthesized at position $\boldsymbol{r} = [r,\ \phi,\ x]^{\mathrm{T}}$ by a continuous cylindrical secondary source with radius r_0 is given as

$$P(\boldsymbol{r},\omega) = \int_0^{2\pi}\int_{-\infty}^{\infty} D(\boldsymbol{r}_0,\omega) G_{\mathrm{3D}}(\boldsymbol{r}-\boldsymbol{r}_0,\omega) r_0 dx_0 d\phi_0, \quad (1)$$

where $\omega = 2\pi f$ denotes the radial frequency, f is the temporal frequency, $D(\boldsymbol{r}_0,\omega)$ is the sound source driving function at position $\boldsymbol{r}_0 = [r_0,\ \phi_0,\ x_0]^{\mathrm{T}}$, and $G_{\mathrm{3D}}(\boldsymbol{r}-\boldsymbol{r}_0,\omega)$ denotes the transfer function of the secondary source placed at $\boldsymbol{r}_0$ to point $\boldsymbol{r}$. Under the free-field assumption, this is the three-dimensional free-field Green's function, defined as

$$G_{\mathrm{3D}}(\boldsymbol{r}-\boldsymbol{r}_0,\omega) = \frac{e^{-jk|\boldsymbol{r}-\boldsymbol{r}_0|}}{4\pi|\boldsymbol{r}-\boldsymbol{r}_0|}, \quad (2)$$

where $j = \sqrt{-1}$, $k = \omega/c$ denotes the wavenumber and c is the speed of sound.

When applying the two-dimensional spatial Fourier transform [21] to (1) with respect to ϕ and x, the convolution along them is performed by the convolution theorem:

$$\tilde{P}_n(r,k_x,\omega) = 2\pi r_0 \tilde{D}_n(k_x,\omega)\tilde{G}_n(r-r_0,k_x,\omega), \quad (3)$$

where k_x denotes the spatial frequency in the direction of x. From [21, 22] and [24], $\tilde{G}_n(r-r_0,k_x,\omega)$ is the two-dimensional spatial Fourier transform of $G_{\mathrm{3D}}(\boldsymbol{x}-\boldsymbol{x}_0,\omega)$ with respect to ϕ and x and is analytically derived as

$$\tilde{G}_n(r-r_0,k_x,\omega)\Big|_{r<r_0} = -\frac{j}{4}H_n^{(2)}(k_r r_0)\,J_n(k_r r), \quad (4)$$

$$\tilde{G}_n(r-r_0,k_x,\omega)\Big|_{r>r_0} = -\frac{j}{4}H_n^{(2)}(k_r r)\,J_n(k_r r_0), \quad (5)$$

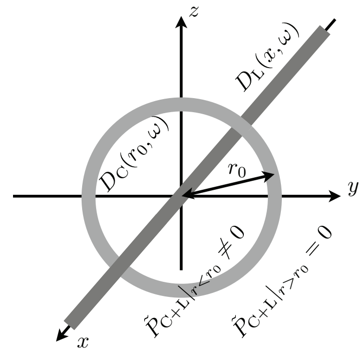

Fig. 2. Proposed near-field sound propagation using circular sound source with radius r_0 centered origin on y-z plane and linear sound source along x-axis. $D_{\mathrm{C}}(r_0,\omega)$ and $D_{\mathrm{L}}(x,\omega)$ are driving functions of circular and linear sound sources analytically derived in (6) and (18). Reproduced sound pressures $\tilde{P}_{\mathrm{C+L}}(r,k_x,\omega)$ for $r > r_0$ and $r < r_0$ are analytically calculated by (16) and (17).

where $k_r = \sqrt{k^2 - k_x^2}$, $H_n^{(2)}$[1] and J_n denote the n-th order Hankel function of the second kind and the n-th order Bessel function of the first kind, respectively [21]. Therefore, $\tilde{G}_n(r-r_0,k_x,\omega)$ is the transfer function in the herical wave spectrum domain from secondary source cylinder r_0 to reproduced cylinder r. (4) and (5) indicate that the propagation property of a cylindrical secondary source with $r < r_0$ is different from that with $r > r_0$.

3. NEAR-FIELD SOUND PROPAGATION USING CIRCULAR AND LINEAR SOUND SOURCES

The foundational concept of the proposed methods is that the sound pressure radiated from a circular sound source outside the circle is canceled out by another linear sound source. To realize this situation, a continuous circular sound source with radius r_0 is centered on the origin on the y-z plane and a continuous linear sound source is located along the x-axis (Fig. 2). This situation can also be realized with cylindrical and linear sources. However, for realistic implementations, the sound source amount should be reduced, and the proposed method introduces a circular source instead of a cylindrical source.

The sound pressure reproduced by linear sound source $P_{\mathrm{L}}(\boldsymbol{r},\omega)$ is radiated axisymmetrically to the x-axis. Then the sound pressure reproduced by circular sound source $P_{\mathrm{C}}(\boldsymbol{r},\omega)$ must also be radiated axisymmetrically to the x-axis. It is apparent that $\tilde{P}_{\mathrm{C},n}(r,k_x,\omega)$ only has a 0-th order component ($n = 0$), and the driving function of a circular source is then

[1] For fitting with the previous research [1], the three-dimensional free-field Green's function is defined in (2) instead of $e^{jk|\boldsymbol{r}-\boldsymbol{r}_0|}/4\pi|\boldsymbol{r}-\boldsymbol{r}_0|$ defined in [21,22]. Then $H_n^{(2)}$ is derived instead of $H_n^{(1)}$ used in [21,22].

independent on ϕ and given as

$$D_{\mathrm{C}}(r_0, \omega) = \begin{cases} 1 & (x = 0) \\ 0 & (x \neq 0). \end{cases} \tag{6}$$

The driving function of a circular source in the helical wave spectrum domain with $n = 0$ is calculated from the spatial Fourier transform to (6) with respect to x. Then $D_C(r_0, \omega)$ just corresponds to delta function $\delta(x)$ in the Fourier transform [21] and is obtained as

$$\tilde{D}_{\mathrm{C},0}(k_x, \omega) = \int_{-\infty}^{\infty} D_{\mathrm{C}}(r_0, \omega) e^{-jk_x x} dx = 1. \tag{7}$$

From (3), (4), (5), and (7), the sound pressure reproduced by a circular source in the helical wave spectrum domain with $n = 0$ is analytically derived as

$$\tilde{P}_{\mathrm{C},0}(r, k_x, \omega)\Big|_{r<r_0} = -\frac{j\pi r_0}{2} H_0^{(2)}(k_r r_0) J_0(k_r r), \tag{8}$$

$$\tilde{P}_{\mathrm{C},0}(r, k_x, \omega)\Big|_{r>r_0} = -\frac{j\pi r_0}{2} H_0^{(2)}(k_r r) J_0(k_r r_0). \tag{9}$$

(8) and (9) also suggest that the propagation property of a circular source for $r < r_0$ is different from that for $r > r_0$. $\tilde{P}_{\mathrm{C},0}(r, k_x, \omega)$ is obviously equivalent to spatial Fourier transform coefficient $\tilde{P}_{\mathrm{C}}(r, k_x, \omega)$ with respect to x and can describe the three-dimensional sound propagation reproduced by a circular source.

In this paragraph, the driving function of linear sound source $D_{\mathrm{L}}(x, \omega)$, which is appropriate for canceling out $\tilde{P}_{\mathrm{C},0}(r, k_x, \omega)|_{r>r_0}$ in (9), is analytically derived. The sound pressure reproduced by a linear source along the x-axis $P_{\mathrm{L}}(\boldsymbol{r}, \omega)$ is also given as

$$P_{\mathrm{L}}(\boldsymbol{r}, \omega) = \int_{-\infty}^{\infty} D_{\mathrm{L}}(\boldsymbol{x}_0, \omega) G_{3\mathrm{D}}(\boldsymbol{r} - \boldsymbol{x}_0, \omega) dx_0. \tag{10}$$

Then, as in (3), the spatial Fourier transform of (10) with respect to x is derived as

$$\tilde{P}_{\mathrm{L}}(r, k_x, \omega) = \tilde{D}_{\mathrm{L}}(k_x, \omega) \tilde{G}_{\mathrm{L}}(r, k_x, \omega), \tag{11}$$

where $\tilde{G}_{\mathrm{L}}(r, k_x, \omega)$ is the transfer function in the wavenumber domain from linear sound source $r = 0$ to reproduced cylinder r [23, 24] and is given as

$$\tilde{G}_{\mathrm{L}}(r, k_x, \omega) = -\frac{j}{4} H_0^{(2)}(k_r r). \tag{12}$$

For canceling $\tilde{P}_{\mathrm{C},0}(r, k_x, \omega)\Big|_{r>r_0}$ in (9) by $\tilde{D}_{\mathrm{L}}(k_x, \omega)$,

$$\tilde{P}_{\mathrm{L}}(r, k_x, \omega) = -\tilde{P}_{\mathrm{C},0}(r, k_x, \omega)\Big|_{r>r_0}, \tag{13}$$

and $\tilde{D}_{\mathrm{L}}(k_x, \omega)$ can be analytically derived by the SDM [23] as

$$\tilde{D}_{\mathrm{L}}(k_x, \omega) = \frac{-\tilde{P}_{\mathrm{C},0}(r, k_x, \omega)}{\tilde{G}_{\mathrm{L}}(r, k_x, \omega)} = -2\pi r_0 J_0(k_r r_0). \tag{14}$$

It is important that $\tilde{D}_{\mathrm{L}}(k_x, \omega)$ is independent on r and

$$\tilde{P}_{\mathrm{L}}(r, k_x, \omega) = \frac{j\pi r_0}{2} H_0^{(2)}(k_r r) J_0(k_r r_0), \tag{15}$$

can be completely reproduced.

Finally, from (9) and (15), the total sound pressure reproduced by both the circular and linear sources for $r > r_0$ is completely canceled out with all r_0 and k_x

$$\begin{aligned} \tilde{P}_{\mathrm{C+L}}(r, k_x, \omega)\Big|_{r>r_0} &= \tilde{P}_{\mathrm{C},0}(r, k_x, \omega)\Big|_{r>r_0} + \tilde{P}_{\mathrm{L}}(r, k_x, \omega) \\ &= 0. \end{aligned} \tag{16}$$

On the other hand, the reproduced sound pressure for $r < r_0$ is calculated from (8) and (15) as

$$\begin{aligned} &\tilde{P}_{\mathrm{C+L}}(r, k_x, \omega)\Big|_{r<r_0} = \tilde{P}_{\mathrm{C},0}(r, k_x, \omega)\Big|_{r<r_0} + \tilde{P}_{\mathrm{L}}(r, k_x, \omega) \\ &= -\frac{j\pi r_0}{2}\left(H_0^{(2)}(k_r r_0) J_0(k_r r) - H_0^{(2)}(k_r r) J_0(k_r r_0)\right). \end{aligned} \tag{17}$$

As a result, (16) and (17) suggest that the proposed method can realize three-dimensional near-field propagation within $r < r_0$ and the propagation distance can be controlled by changing the radius of circular source r_0.

To calculate stable driving signals, $\tilde{D}_{\mathrm{L}}(k_x, \omega) = 0$ for $k_r^2 = k^2 - k_x^2 < 0$, corresponding to the evanescent wave components [22]. Then, the inverse spatial Fourier transform of (14) is analytically calculated from the relation of (3.876-1) in [24] and given as

$$D_{\mathrm{L}}(x, \omega) = -2r_0 \frac{\sin\left(k\sqrt{x^2 + r_0^2}\right)}{\sqrt{x^2 + r_0^2}} \qquad (|k| > |k_x|). \tag{18}$$

In a practical implementation, a circular and a linear array of loudspeakers is used instead of continuous circular and linear sound sources. Then (6) and (18) must be discretized and (18) must be truncated.

4. EXPERIMENTS

Computer simulations were conducted to evaluate the proposed method. In all the calculations, speed of sound c was 343.26 m/s and a three-dimensional free-field was assumed.

For a realistic implementation, the channel numbers of the circular and linear arrays were M=32 and N=64, respectively. The distance between the adjacent loudspeakers of the linear array was Δx=0.05 m.

Figs 3(a) to (c) show the results of the sound pressures reproduced by a circular array, a linear array and both arrays, respectively. The radius of the circular array is r_0=0.25 m, and $f = 1$ kHz. These results suggest that the propagated sound pressure by circular array $P_{\mathrm{C}}(\boldsymbol{r}, \omega)$ for $r > r_0$ is reproduced by a linear array with antiphase as $P_{\mathrm{L}}(\boldsymbol{r}, \omega)$, and the

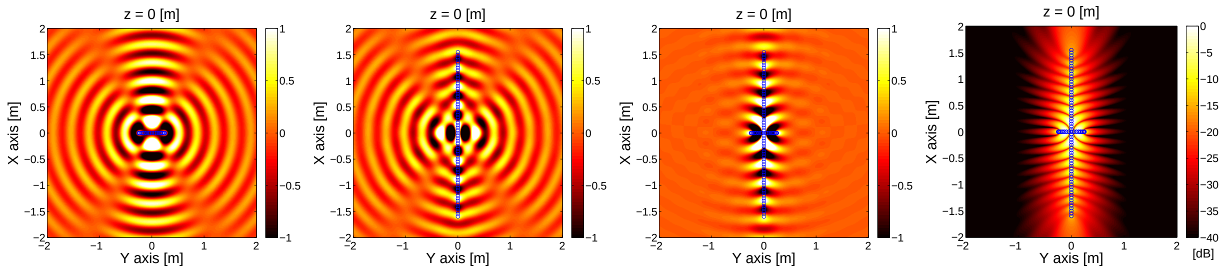

(a) $\Re\{P_{\mathrm{C}}(\boldsymbol{r},\omega)\}$ (b) $\Re\{P_{\mathrm{L}}(\boldsymbol{r},\omega)\}$ (c) $\Re\{P_{\mathrm{C+L}}(\boldsymbol{r},\omega)\}$ (d) $20\log_{10}|P_{\mathrm{C+L}}(\boldsymbol{r},\omega)|$

Fig. 3. Results of (a)-(c) reproduced sound pressure and (d) sound pressure level with radius of circular array r_0=0.25 m for f=1 kHz. $\Re\{\cdot\}$ denotes complex number's real part. Blue circles are loudspeakers. Channel numbers of circular and linear arrays are M=32 and N=64. Distance between adjacent loudspeakers of linear array is Δx=0.05 m. Sound pressure level at $\boldsymbol{r} = [0.1,\ 0,\ 0]^{\mathrm{T}}$ is set to 0 dB in (d).

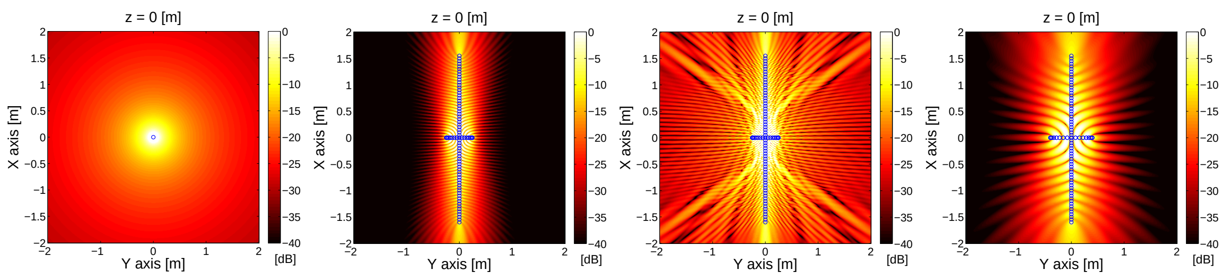

(a) Monopole (b) f=3 kHz, r_0=0.25 m (c) f=5 kHz, r_0=0.25 m (d) f=1 kHz, r_0=0.4 m

Fig. 4. Results of sound pressure level $20\log_{10}|P(\boldsymbol{r},\omega)|$ reproduced by (a) monopole point source and (b)-(d) proposed method with M=32, N=64, and Δx=0.05 m. Blue circles are loudspeakers. Sound pressure level at $\boldsymbol{r} = [0.1,\ 0,\ 0]^{\mathrm{T}}$ is set to 0 dB.

total reproduced sound pressure can be efficiently canceled at $r > r_0$.

The results of the sound pressure level of the total reproduced sound by the proposed method are depicted in Figs. 3(d) and 4(b) to (d) and compared with that of a monopole point source shown in Fig. 4(a). Especially for f=3 kHz in Fig. 4(b), these results indicate that the proposed method can realize near-field propagation $P_{\mathrm{L+C}}(\boldsymbol{r},\omega)$ within $r < r_0$ relative to a monopole. Moreover, the results in Fig. 3(d) for r_0=0.25 m and in Fig. 4(d) for r_0=0.4 m suggest that the propagation distance can be controlled by changing the radius of a circular array.

The reproduced sound pressures for f=1 kHz in Fig. 3(d) and in Fig. 4(d), however, are slightly radiated at $r > r_0$. These artifacts are caused by the effects of the truncation of a linear array and discarding the evanescent component because these effects are not negligible at low frequency. In addition, the reproduced sound pressure for f=5 kHz in Fig. 4(c) is obviously radiated at $r > r_0$ by spatial aliasing because the spatial Nyquist frequency of both arrays is about 3.4 kHz.

5. CONCLUSION

This paper proposed a novel three-dimensional near-field sound propagation method whose elementary concept is that the sound pressure radiated from a circular sound source outside the circle is perfectly canceled out using a linear sound source. For describing three-dimensional sound propagation by a circular sound source, a reproduced sound field by a cylindrical secondary source was firstly introduced. Then the adequate arrangement of circular and linear sound sources was proposed and the appropriate driving functions of both sources and the three-dimensional reproduced sound pressures were analytically derived. Not only the analytically derived total sound pressures reproduced by both sources but also the computer simulation results indicated that the proposed method realizes effective three-dimensional near-field sound propagation and the propagation distance can be controlled by changing the radius of a circular sound source.

Future work will apply the proposed method in actual environments and conduct implementations and evaluations in reverberant environments.

6. REFERENCES

[1] T. Okamoto, "Generation of multiple sound zones by spatial filtering in wavenumber domain using a linear array of loudspeakers," in *Proc. ICASSP*, May 2014, pp. 4733–4737.

[2] T. Betlehem, W. Zhang, M. Poletti, and T. Abhayapala, "Personal sound zones: Delivering interface-free audio to multiple listeners," *IEEE Signal Process. Mag.*, vol. 32, no. 2, pp. 81–91, Mar. 2015.

[3] W. F. Druyvesteyn and J. Garas, "Personal sound," *J. Audio Eng. Soc.*, vol. 45, no. 9, pp. 685–701, Sept. 1997.

[4] J.-H. Chang, C.-H. Lee, J.-Y. Park, and Y.-H. Kim, "A realization of sound focused personal audio system using acoustic contrast control," *J. Acoust. Soc. Am.*, vol. 125, no. 4, pp. 2091–2097, Apr. 2009.

[5] S. J. Elliott, J. Cheer, J.-W. Choi, and Y. Kim, "Robustness and regularization of personal audio systems," *IEEE Trans. Audio, Speech, Lang. Process.*, vol. 20, no. 7, pp. 2123–2133, Sept. 2012.

[6] Y. Cai, M. Wu, and J. Yang, "Sound reproduction in personal audio systems using the least-squares approach with acoustic contrast control constraint," *J. Acoust. Soc. Am.*, vol. 135, no. 2, pp. 734–741, Feb. 2014.

[7] J.-W. Choi and Y.-H. Kim, "Generation of an acoustically bright zone with an illuminated region using multiple sources," *J. Acoust. Soc. Am.*, vol. 111, no. 4, pp. 1695–1700, Apr. 2002.

[8] M. Shin, S. Q. Lee, F. M. Fazi, P. A. Nelson, D. Kim, S. Wang, K. H. Park, and J. Seo, "Maximization of acoustic energy difference between two spaces," *J. Acoust. Soc. Am.*, vol. 128, no. 1, pp. 121–131, July 2010.

[9] P. Coleman, P. J. B. Jackson, M. Olik, M. Møller, M. Olsen, and J. A. Pedersen, "Acoustic contrast, planarity and robustness of sound zone methods using a circular loudspeaker array," *J. Acoust. Soc. Am.*, vol. 135, no. 4, pp. 1929–1940, Apr. 2014.

[10] M. Shin, F. M. Fazi, P. A. Nelson, and F. C. Hirono, "Controlled sound field with a dual layer loudspeaker array," *J. Sound Vib.*, vol. 333, no. 16, pp. 3794–3817, Aug. 2014.

[11] M. Poletti, "An investigation of 2d multizone surround sound systems," in *Proc. 125th Conv. Audio Eng. Soc.*, Oct. 2008.

[12] Y. J. Wu and T. D. Abhayapala, "Spatial multizone soundfield reproduction: theory and design," *IEEE Trans. Audio, Speech, Lang. Process.*, vol. 19, no. 6, pp. 1711–1720, Aug. 2011.

[13] M. Møller, M. Olsen, and F. Jacobsen, "A hybrid method combining synthesis of a sound field and control of acoustic contrast," in *Proc. 132nd Conv. Audio Eng. Soc.*, Apr. 2012.

[14] N. Radmanesh and I. S. Burnett, "Generation of isolated wideband sound fields using a combined two-stage lasso-ls algorithm," *IEEE Trans. Audio, Speech, Lang. Process.*, vol. 21, no. 2, pp. 378–387, Feb. 2013.

[15] W. Jin, W. B. Kleijn, and D. Virette, "Multizone soundfield reproduction using orthogonal basis expansion," in *Proc. ICASSP*, May 2013, pp. 311–315.

[16] W. Jin and W. B. Kleijn, "Multizone soundfield reproduction in reverberant rooms using compressed sensing techniques," in *Proc. ICASSP*, May 2014, pp. 4728–4732.

[17] H. Itou, K. Furuya, and Y. Haneda, "Evanescent wave reproduction using linear array of loudspeakers," in *Proc. WASPAA*, Oct. 2011, pp. 37–40.

[18] H. Itou, K. Furuya, and Y. Haneda, "Localized sound reproduction using circular loudspeaker array based on acoustic evanescent wave," in *Proc. ICASSP*, Mar. 2012, pp. 221–224.

[19] J.-H. Chang and F. Jacobsen, "Sound field control with a circular double-layer array of loudspeaker," *J. Acoust. Soc. Am.*, vol. 131, no. 6, pp. 4518–4525, June 2012.

[20] J.-H. Chang and F. Jacobsen, "Experimental validation of sound field control with a circular double-layer array of loudspeakers," *J. Acoust. Soc. Am.*, vol. 133, no. 4, pp. 2046–2054, Apr. 2013.

[21] E. G. Williams, *Fourier Acoustics: Sound Radiation and Nearfield Acoustic Holography*, Academic Press, San Diego, 1999.

[22] S. Koyama, K. Furuya, Y. Hiwasaki, Y. Haneda, and Y. Suzuki, "Wave field reconstruction filtering in cylindrical harmonic domain for with-hight recording and reproduction," *IEEE/ACM Trans. Audio, Speech, Lang. Process.*, vol. 22, no. 10, pp. 1546–1557, Oct. 2014.

[23] J. Ahrens and S. Spors, "Sound field reproduction using planar and linear arrays of loudspeakers," *IEEE Trans. Audio, Speech, Lang. Process.*, vol. 18, no. 8, pp. 2038–2050, Nov. 2010.

[24] I. S. Gradshteyn and I. M. Ryzhik, *Table of Integrals, Series, and Products*, Academic Press, New York, 2007.